J|A|C|S ARTICLES

Published on Web 07/30/2009

# Quantum Mechanical Design and Structure of the $Li@B_{10}H_{14}$ Basket with a Remarkably Enhanced Electro-Optical Response

Shabbir Muhammad, Hongliang Xu, Yi Liao, Yuhe Kan, and Zhongmin Su*

*Institute of Functional Material Chemistry, Faculty of Chemistry, Northeast Normal University, Changchun 130024, People's Republic of China*

Received April 22, 2009; E-mail: zmsu@nenu.edu.cn

***Abstract:*** An innovative type of lithium decahydroborate ($Li@B_{10}H_{14}$) complex with a basketlike complexant of decaborane ($B_{10}H_{14}$) has been designed using quantum mechanical methods. As Li atom binds in a handle fashion to terminal electrophilic boron atoms of the decaborane basket, its NBO charge $q$ (Li) is found to be 0.876, close to +1. This shows that the Li atom has been ionized to form a cation and an anion at the open end of $B_{10}H_{14}$. The most fascinating feature of this Li doping is its loosely bound valence electron, which has been pulled into the cavity of the $B_{10}H_{14}$ basket and become diffuse by the electron-deficient morphological features of the open end of the $B_{10}H_{14}$ basket. Strikingly, the first hyperpolarizability ($\beta_0$) of $Li@B_{10}H_{14}$ is about 340 times larger than that of $B_{10}H_{14}$, computed to be 23 075 au ($199 \times 10^{-30}$ esu) and 68 au, respectively. Besides this, the intercalation of the Li atom to the $B_{10}H_{14}$ basket brings some distinctive changes in its Raman, $^{11}B$ NMR, and UV−vis spectra along with its other electronic properties that might be used by the experimentalists to identify this novel kind of $Li@B_{10}H_{14}$ complex with a large electro-optical response. This study may evoke the possibility to explore a new thriving area, i.e., alkali metal−boranes for NLO application.

## Introduction

A large number of reports have been presented up until now on nonlinear optical (NLO) materials with different conventional strategies to enhance the NLO response.[1] These strategies mainly include the use of molecules with extended $\pi$-electron systems,[2a,b] the planar donor−$\pi$-conjugated bridge−acceptor (D−$\pi$−A) model,[2c,d] twisted $\pi$-electron systems,[2e] octupolar molecules,[3a−c] enhanced push−pull effects,[3d,e] bond length alternation (BLA) theory,[4a] incorporation of ligated metal into the organic compounds,[4b−e] and so forth. Similarly, Li and co-workers have made many fascinating reports on NLO material with Li-doped electride/salt complexes.[5] These alkali-metal-doped complexes have shown a significantly large NLO response, and the Li valence electron played a crucial role in the large NLO value of these compounds. These reports mainly described the electride or alkalide complexes, composed of alkali-metal atoms intercalated within the cages formed of one or two organic

(1) (a) Kirtman, B.; Champagne, B.; Bishop, D. M. *J. Am. Chem. Soc.* **2000**, *122*, 8007–8012. (b) Champagne, B.; Spassova, M.; Jadin, J. B.; Kirtman, B. *J. Chem. Phys.* **2002**, *116*, 3935–3946. (c) Marder, S. R.; Torruellas, W. E.; Blanchard, D. M.; Ricci, V.; Stegeman, G. I.; Gilmour, S.; Bredas, J. L.; Li, J.; Bublitz, G. U.; Boxer, S. G. *Science* **1997**, *276*, 1233–1236. (d) Avramopoulos, A.; Reis, H.; Li, J.; Papadopoulos, M. G. *J. Am. Chem. Soc.* **2004**, *126*, 6179–6184. (e) Le Bouder, T.; Maury, O.; Bondon, A.; Costuas, K.; Amouyal, E.; Ledoux, I.; Zyss, J.; Le Bozec, H. *J. Am. Chem. Soc.* **2003**, *125*, 12884–12899. (f) Clays, K.; Wostyn, K.; Persoons, A.; Stefano, M. B.; Maiorana, S.; Papagni, A.; Daul, C. A.; Weber, V. *Chem. Phys. Lett.* **2003**, *372*, 438–442. (g) Coe, B. J.; Harris, J. A.; Asselberghs, I.; Clays, K.; Olbrechts, G.; Persoons, A.; Hupp, J. T.; Johnson, R. C.; Coles, S. J.; Hursthouse, M. B.; Nakatani, K. *Adv. Funct. Mater.* **2002**, *12*, 110–116. (h) Datta, A. *J. Phys. Chem. C* **2009**, *113*, 3339–3344.

(2) (a) Marder, S. R.; Gorman, C. B.; Meyers, F.; Perry, J. W.; Bourhill, G.; Bredas, J. L.; Pierce, B. M. *Science* **1994**, *265*, 632–635. (b) Blanchard, D. M.; Alain, V.; Bedworth, P. V; Marder, S. R.; Fort, A.; Runser, C.; Barzoukas, M.; Lebus, S.; Wortmann, R. *Chem.—Eur. J.* **1997**, *3*, 1091–1104. (c) Zyss, J.; Ledoux, I. *Chem. Rev.* **1994**, *94*, 77. (d) Janjua, M. R. S. A.; Liu, C. G.; Guan, W.; Zhuang, J.; Muhammad, S.; Yan, L. K.; Su, Z. M. *J. Phys. Chem. A* **2009**, *113*, 3576. (e) Yang, J. S.; Liau, K. L.; Li, C. Y.; Chen, M. Y. *J. Am. Chem. Soc.* **2007**, *129*, 13183.

(3) (a) Maury, O.; Viau, L.; Senechal, K.; Corre, B.; Guegan, J. P.; Renouard, T.; Ledoux, I.; Zyss, J.; Bozec, L. H. *Chem.—Eur. J.* **2004**, *10*, 4454–4466. (b) Lee, M. J.; Piao, M.; Jeong, M. Y.; Lee, S. H.; Kang, K. M.; Jeon, S. J.; Tong, G. L. B.; Cho, B. R. *J. Mater. Chem.* **2003**, *13*, 1030–1037. (c) Lee, S. H.; Park, J. R.; Jeong, M. Y.; Kim, H. M.; Li, S. J.; Song, J.; Ham, S.; Jeon, S. J.; Cho, B. R. *ChemPhysChem* **2006**, *7*, 206–212. (d) Coe, B. J.; Jones, L. A.; Brunschwig, B. S.; Asselberghs, I.; Clays, K.; Persoons, A. *J. Am. Chem. Soc.* **2003**, *125*, 862–863. (e) Coe, B. J.; Foxon, S. P.; Harper, E. C.; Raftery, J.; Shaw, R.; Swanson, C. A.; Asselberghs, I.; Clays, K.; Brunschwig, B. S.; Fitch, A. G. *Inorg. Chem.* **2009**, *48*, 1370–1379.

(4) (a) Meyers, F.; Marder, S. R.; Pierce, B. M.; Bredas, J. L. *J. Am. Chem. Soc.* **1994**, *116*, 10703–10714. (b) Bella, S. D. *Chem. Soc. Rev.* **2001**, *30*, 355–366. (c) Lacroix, P. G. *Eur. J. Inorg. Chem.* **2001**, *33*, 9–348. (d) Coe, B. J. *Acc. Chem. Res.* **2006**, *39*, 383–393. (e) Kanis, D. R.; Ratner, M. A.; Marks, T. J. *Chem. Rev.* **1994**, *94*, 195–242.

(5) (a) Jing, Y. Q.; Li, Z. R.; Wu, D.; Li, Y.; Wang, B. Q. *J. Phys. Chem. B* **2006**, *110*, 11725–11729. (b) Chen, W.; Li, Z. R.; Wu, D.; Li, Y.; Sun, C. C.; Gu, F. L. *J. Am. Chem. Soc.* **2005**, *127*, 10977–10981. (c) Li, Z. J.; Li, Z. R.; Wang, F. F; Luo, C.; Ma, F.; Wu, D.; Wang, Q.; Huang, X. R. *J. Phys. Chem. A* **2009**, *113*, 2961–2966. (d) Xu, H. L.; Li, Z. R.; Wu, D.; Ma, F.; Li, Z. J. *J. Phys. Chem. C* **2009**, *113*, 4984–4986. (e) Chen, W.; Li, Z. R.; Wu, D; Li, Y.; Sun, C. C. *J. Phys. Chem. A* **2005**, *109*, 2920–2924. (f) Xu, H. L.; Li, Z. R.; Wu, D.; Wang, B. Q; Li, Y.; Gu, F. L.; Aoki, Y. *J. Am. Chem. Soc.* **2007**, *129*, 2967–2970. (g) Chen, W.; Li, Z. R.; Wu, D.; Li, R. Y.; Sun, C. C. *J. Phys. Chem. B* **2005**, *109*, 601–608. (h) Ma, F.; Li, Z. R.; Xu, H. L.; Li, Z. J.; Li, Z. S.; Aoki, Y.; Gu, F. L. *J. Phys. Chem. A* **2008**, *112*, 11462–11467. (i) Chen, W.; Li, Z. R.; Wu, D.; Li, Y.; Sun, C. C.; Gu, F. L.; Aoki, Y. *J. Am. Chem. Soc.* **2006**, *128*, 1072–1073. (j) Wang, F. F.; Li, Z. R.; Wu, D; Wang, B. Q.; Li, Y; Li, Z. J.; Chen, W.; Yu, G. T.; Gu, F. L.; Aoki, Y. *J. Phys. Chem. B* **2008**, *112*, 1090–1094.

  

complexants except for the only inorganic $Li(NH_3)_nNa$ complex,[5a] with a flexibly coordinated sphere of $NH_3$ molecules. In designing these new electride complexes with large first hyperpolarizabilities, usually organic complexants such as crown ethers,[5b] cyclic polyamines,[5c] tubiform cyclacene,[5d] hydrocarbons,[5e] and fluorocarbons,[5f] etc. have been used up until now. In spite of these valuable reports, still there is no experimental evidence to separate the above-mentioned Li complexes with large NLO values, which might be due to the instability of these organic complexants and/or inadequate reactivity of the Li atom caused by the presence of some repulsive interaction between the Li electron and these organic complexants.[5a−h] Among these NLO electride complexes, of particular importance to the present work are $(HCN)_n$ ($n = 1$, 2, 3) chain clusters, doped with a Li atom. In $(HCN)_n$ the terminal H atom is an electron-pulling group; as the Li atom interacts with the terminal H atom, the 2s electron of the Li atom is pulled toward the H atom, which results in a relatively stable electride of $Li\cdots(HCN)_n$ with $Li^+$ and a Redberg-like diffuse 2s electron.[5g] Similarly, Dye et al.[6] described a way to make stable alkali-metal electrides by using inorganic complexants, which are resistant to thermal decomposition at room temperature due to the absence of oxygen−carbon bonds. From the above reports and appealing features of rigid inorganic complexants, we were inspired to probe into the research of novel inorganic alkali-metal complexes with a large NLO response. We first focus on the rigid borane clusters as complexants to design a new type of alkali-metal complexes with a large NLO value. Our study is different from the previous studies[5] because we used rigid inorganic borane clusters without a weak flexible configuration. The most innovative and diverse feature of this complex is its loosely bound Li valence electron, which is diffused and polarized into the cavity of the $B_{10}H_{14}$ basket under the action of four electron-deficient terminal H atoms and two electron-deficient terminal boron atoms. Unlike the previous Li complexes,[5a−h] where the Li valence electron had been pushed out by the repulsive forces of N or F lone pair electrons of organic complexants, the inward pull in the present complex can offer greater stability to the Li diffuse electron. This doping of Li with the borane cluster might give a room temperature stable complex in experimental work with a large NLO response.

Compounds of boranes and borides indeed have spanned a large area of chemistry[7] due to their aesthetically appealing structures and unique bonding features[8] and the formation of cages and clusters.[9] Among the borides, lithium borides have been extensively studied and showed that the lithium atom preferably forms a bridge around the central B−B bond.[9b] Similarly, Wasczcak et al. have synthesized tricarbadecaboranyl analogues in which Li is the center over the six-membered open face of the carbaborane cage and is solvated by two acetonitrile molecules.[10] Boranes can also form metal−hydrogen−boron

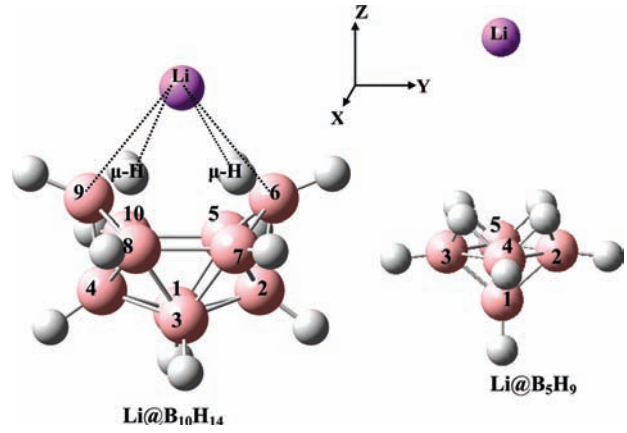


***Figure 1.*** Labeled diagrams of $Li@B_{10}H_{14}$ and $Li@B_5H_9$.

(MHB) bonds with metals (H is a bridging atom). The bridging hydrogen participates most often in a multicenter two-electron bond both within the cluster and in the interaction with metals. These hydrogens are distinctly protonic, and their relative acidity depends on the cage size as well as other parameters.[11] Among the boranes, deca- and pentaboranes are the most stable *nido*-boranes. Decaborane with double the number of boron atoms compared to pentaborane[12] is in the shape of a basket, a very useful starting material for a lot of borane chemistry.[13] Self-consistent field calculations[14a] of the electron density for $B_{10}H_{14}$ showed clearly that the order from least negative (most positive) to most negative is B(6,9), B(5,7,8,10), B(1,3), and B(1,4) (see Figure 1 for labeling). The positive charge at the open face of $B_{10}H_{14}$, i.e., B(6,9) and B(5,7,8,10), has been elegantly demonstrated by the structure of the charge-transfer $B_{10}H_{14}I^-$ complex, in which the negatively charged $I^-$ sits on this open face.[15c] This $B_{10}H_{14}$ (basket) exhibits a wide range of properties, and its complexes with ions and atoms have been studied by experimentally[15] and theoretically.[14b] In light of the above evidence, in our present work, we selected borane clusters to dope with lithium. Decaborane showed an effective interaction with the lithium atom due to the larger cage size and higher dipolar character as proved in subsequent sections and also in the Supporting Information. In this alkali-metal−borane cluster, the Li atom showed a high degree of ionicity that might be due to the pulling of the loosely bound valence electron of the Li atom toward the polar end of the borane cluster, which subsequently has become diffuse and easily excited. Since this is the key factor in the formation of Li organic electrides with

(6) (a) Dye, J. L. *Inorg. Chem.* **1997**, *36*, 3816–3826. (b) Ichimura, A. S.; Dye, J. L. *J. Am. Chem. Soc.* **2002**, *124*, 1170–1171. (c) Dye, J. L. *Science* **2003**, *301*, 607–608.
(7) (a) Hawthorne, M. F. *Angew. Chem., Int. Ed. Engl.* **1993**, *32*, 950–984. (b) Hnyk, D.; Holub, J.; Hayes, S. A.; Robinson, M. F.; Wann, D. A.; Robertson, H. E.; Rankin, D. W. H. *Inorg. Chem.* **2006**, *45*, 8442–8446.
(8) (a) Colquhoun, H. M.; Lewis, D. F.; Herbertson, P. L.; Wade, K. *Polymer* **1997**, *38*, 4539–4546. (b) Hong, E.; Kim, Y.; Do, Y. *Organometallics* **1998**, *17*, 2933–2935.
(9) (a) Nguyen, K. A.; Lammertsma, K. *J. Phys. Chem. A* **1998**, *102*, 1608–1614. (b) Srinivas, G. N.; Hamilton, T. P.; Boatz, J. A.; Lammertsma, K. *J. Phys. Chem. A* **1999**, *103*, 9931–9937.
(10) Wasczcak, M. D.; Wang, Y.; Garg, A.; Geiger, W. E.; Kang, S. O.; Patrick, J.; Carroll, P. J.; Sneddon, L. G. *J. Am. Chem. Soc.* **2001**, *123*, 2783–2790.
(11) (a) Williams, R. E. *Adv. Inorg. Chem. Radiochem.* **1976**, *18*, 67–142. (b) Gaines, D. F. *Acc. Chem. Res.* **1973**, *6*, 416–421. (c) Parry, R. W.; Edwards, L. J. *J. Am. Chem. Soc.* **1959**, *81*, 3554–3560.
(12) Brain, P. T.; Hnykt, D.; Rankins, D.W. H.; Buhl, M.; Schleyer, P. V. R. *Polyhedron* **1994**, *13*, 1453–1466.
(13) Stanko, V. I.; Chapovskii Yu, A.; Brattsev, V. A.; Zakharkin, L. I. *Russ. Chem. Rev.* **1965**, *34*, 424–439.
(14) (a) Laws, E. A.; Stevens, R. M.; Lipscomb, W. N. *J. Am. Chem. Soc.* **1972**, *94*, 4467–4474. (b) Sioutis, I.; Pitzer, R. M. *J. Phys. Chem. A* **2006**, *110*, 12528–12534.
(15) (a) Gaines, D. F. *Inorg. Chem.* **2000**, *39*, 1812–1813. (b) Kasper, J. S.; Lucht, C. M.; Harker, D. *Acta Crystallogr.* **1950**, *3*, 436–455. (c) Wermer, J. R.; Hollander, O.; Huffman, J. C.; Bauer, J. A. K.; Dou, D.; Hsu, L. Y.; Leussing, D. L.; Shore, S. G. *Inorg. Chem.* **1995**, *34*, 3065–3071. (d) Keller, W. E.; Johnston, H. L. *J. Chem. Phys.* **1952**, *20*, 1749–1751. (e) Pimentel, G. C.; Pitzer, K. S. *J. Chem. Phys.* **1949**, *17*, 882–884. (f) Ionov, S. P.; Kuznetsov, N. T. *Russ. J. Coord. Chem.* **2005**, *31*, 138–141.

large NLO values, our work may provide a novel idea to design new stable materials with large electro-optical properties.

## Computational Details

The geometries of $B_{10}H_{14}$ and $B_5H_9$ and their Li complexes have been optimized with all real frequencies by using the Møller−Plesset (MP2) method. All open-shell calculations were performed using unrestricted methods (UMP2), and spin contamination was found to be very small, less than 1.80% from the exact expected value. The coupled-cluster theory with both single and double substitutions (CCSD) has also been used to compare the MP2 level geometries with higher level methods. The first hyperpolarizabilities are evaluated by finite field (FF) approach at the MP2 level. In many reports,[5a,c−h,j] the MP2 method is considered to be the most suitable method for calculating the first hyperpolarizability. The reason is that with acceptable computation costs, the MP2 results are also very close to those obtained from the more complicated correlation methods (for example, QCISD[5g]). The 6-31+G* basis set is employed for all calculations. This basis set is found to be satisfactory for the calculation of first hyperpolarizabilities and transition energies as explained in the Supporting Information. The magnitude of the applied electric field is chosen as 0.001 au for the calculation of the hyperpolarizability, which has been proved to be the most adequate value for the numerical differentiation in several similar studies.[5] The magnetic shieldings were calculated on optimized geometries by employing gauge-including atomic orbitals (GIAOs) with the MP2/6-31+G* level of theory. Several reports of Rasul et al.[16] have demonstrated that the GIAO-MP2 method can give reliable results for $^{11}$B NMR chemical shift calculations. The $^{11}$B NMR chemical shifts were first computed with $B_2H_6$ [the calculated absolute shift, i.e., $\sigma$(B), is 103.9] as a reference, which is in accordance with previous (GIAO-MP2) calculations.[17] The $^{11}$B NMR chemical shifts were finally referenced to $BF_3{\cdot}OEt_2$ [$\delta(B_2H_6) = 16.6$ vs $BF_3{\cdot}OEt_2$].[16b] Furthermore, the excellent coupling of theoretical and experimental results gives credit to the choice of method and basis set in this study. In the FF method when a molecule is subjected to the static electric field ($F$), the energy ($E$) of the molecule is expressed by

$$E = E^{(0)} - \mu_1 F_1 - \frac{1}{2}\alpha_{ij}F_iF_j - \frac{1}{6}\beta_{ijk}F_iF_jF_k - \frac{1}{24}\gamma_{ijkl}F_iF_jF_kF_l - \ldots \quad (1)$$

where $E^{(0)}$ is the energy of the molecule in the absence of an electronic field, $\mu$ is the component of the dipole moment vector,$\alpha$ is the linear polarizability tensor, $\beta$ and $\gamma$ are the first and second hyperpolarizability tensors, respectively, and $i$, $j$, and $k$ label the $x$, $y$, and $z$ components, respectively. For a molecule, the average dipole moment ($\mu_0$) and polarizability ($\alpha_0$) are defined as follows:

$$\mu_0 = (\mu_x^2 + \mu_y^2 + \mu_z^2)^{1/2} \quad (2)$$

$$\alpha_0 = \frac{1}{3}(\alpha_{xx} + \alpha_{yy} + \alpha_{zz}) \quad (3)$$

The first hyperpolarizability is defined as

$$\beta_0 = (\beta_x^2 + \beta_y^2 + \beta_z^2)^{1/2} \quad (4)$$

where

$$\beta_i = \frac{3}{5}(\beta_{iii} + \beta_{ijj} + \beta_{ikk}) \qquad i,j,k = x,y,z \quad (5)$$

All the calculations were performed using the Gaussian 03 program package.[18]

## Results and Discussion

**Geometries of Stationary Points.** The structure of decaborane is well-known, and we have adopted similar structural parameters as they have been explained in the previous theoretical[14] and experimental[15] work. Different conformations have been considered for the placement of the Li atom, i.e., above the terminal boron atoms 6 and 9 and in the center of the $B_{10}H_{14}$ basket. The conformation of $B_{10}H_{14}$ with the Li atom in the center with $C_{2v}$ symmetry is found to be the most stable (see Figure 1).

The structure of lithium decahydroborate (Li@$B_{10}H_{14}$) resembles a basket, and the Li atom merely forms the handle of this basket. In this basketlike molecule, the Li atom is located along the principal $C_2$ axis in a bridging fashion with a distance of 2.707 Å from the two terminal boron atoms ($B_6$, $B_9$), while from four bridging hydrogen atoms ($\mu$-H) this distance is 2.132 Å. These distances are much shorter than the sums of the van der Waals radii of the B, Li and B, H atoms, which are 3.82 and 2.91 Å,[19] respectively. These distances present an effective interaction between the Li atom and open face of the $B_{10}H_{14}$ basket. The main geometrical parameters of $B_{10}H_{14}$ and Li@$B_{10}H_{14}$ are listed in Table 1.

The largest change in distance is observed between $B_6$ and $B_9$ atoms at the open face of $B_{10}H_{14}$; the distance between $B_6$ and $B_9$ atoms becomes shorter by 0.110 Å after the interaction with the Li atom. The change of the distance in bridging hydrogen atoms is also important, with 0.071 Å from the lower rim of four bridged boron atoms toward the Li atom. Unlike the Li@$B_{10}H_{14}$ basket, in Li@$B_5H_9$ the interaction between the Li atom and $B_5H_9$ is not significant. This is reflected in the 1.31 and 1.39 Å larger distances between the Li atom and B and H atoms of the $B_5H_9$ molecule, respectively, as compared to the sum of their van der Waals radii. The NBO charge analysis is also in line with the above observations. As the Li atom binds to $B_{10}H_{14}$, its NBO charge $q$(Li) is found to be 0.876, close to +1, which shows that the Li atom has been ionized to form a cation and an anion at the open face of the $B_{10}H_{14}$ basket (see Figure 2), whereas in the case of Li@$B_5H_9$, there is no change

***Table 1.*** Geometrical Parameters (Å) of $B_{10}H_{14}$ and Li@$B_{10}H_{14}$ at the MP2/6-31+G* Level of Theory

| bond | $B_{10}H_{14}$(exptl) [a] | $B_{10}H_{14}$ [b] | $B_{10}H_{14}$ | Li@$B_{10}H_{14}$ |
|---|---|---|---|---|
| $B_5-B_2$ | 1.74 ± 0.03 | 1.789 | 1.785 | 1.787 |
| $B_5-B_6$ | 1.76 ± 0.03 | 1.786 | 1.780 | 1.849 |
| $B_5-B_1$ | 1.74 ± 0.02 | 1.749 | 1.749 | 1.753 |
| $B_2-B_1$ | 1.79 ± 0.04 | 1.781 | 1.778 | 1.780 |
| $B_6-B_2$ | 1.73 ± 0.04 | 1.724 | 1.722 | 1.750 |
| $B_6-B_7$ | 1.78 ± 0.03 | 1.786 | 1.780 | 1.849 |
| $B_7-B_3$ | 1.74 ± 0.02 | 1.749 | 1.749 | 1.753 |
| $B_1-B_3$ | 1.78 ± 0.02 | 1.776 | 1.774 | 1.740 |
| $B_9-B_6$ | | 3.592 | 3.582 | 3.472 |
| $B_7-B_5$ | | 2.837 | 2.829 | 2.886 |
| $B_7-B_8$ | 2.01 ± 0.02 | 1.989 | 1.988 | 1.861 |
| $B_9-\mu$-$H_9$ | 1.40 ± 0.05 | 1.333 | 1.333 | 1.306 |
| $B_8-\mu$-$H_9$ | 1.34 ± 0.05 | 1.322 | 1.319 | 1.390 |
| $B_9-H_9$ | 1.25 ± 0.05 | 1.190 | 1.188 | 1.191 |
| $B_9-Li$ | | | | 2.707 |
| $\mu$-$H_9-Li$ | | | | 2.132 |

[a] For experimental data see ref 15b. [b] At the CCSD/6-31+G* level of theory.

(16) (a) Rasul, G.; Prakash, G. K. S.; Olah, G. A. *Inorg. Chem.* **1999**, *38*, 44–47. (b) Rasul, G.; Prakash, G. K. S.; Olah, G. A. *Natl. Acad. Sci. U.S.A.* **2002**, *99*, 9635–9638.
(17) Buhl, M.; Gauss, J.; Hofman, M.; Schleyer, P. V. R. *J. Am. Chem. Soc.* **1993**, *115*, 12385–12390.

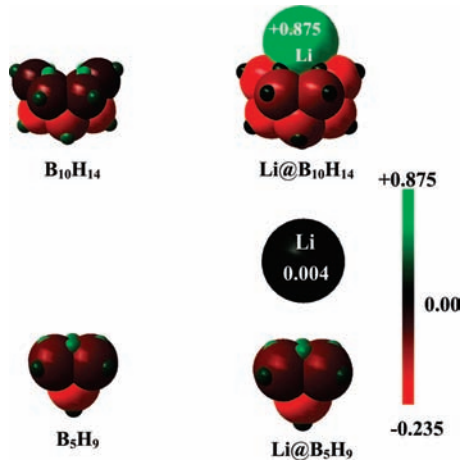


***Figure 2.*** NBO charges of $Li@B_{10}H_{14}$ and $Li@B_5H_9$ with MP2/6-31+G* at scaled van der Waals radii.

***Table 2.*** Raman Spectral Data of $B_{10}H_{14}$ and $Li@B_{10}H_{14}$

| freq(calcd) ($cm^{-1}$) | freq(exptl)[a] ($cm^{-1}$) | Raman activity (au) | mode assignment |
|---|---|---|---|
| | | $B_{10}H_{14}$ | |
| 339 | 350 (S) | 8 | B−B skeleton bending |
| 696 | 709 (S) | 50 | B−H bending ∥ $C_2$ axis |
| 861 | 858 (S) | 40 | B−H bending ⊥ $C_2$ axis |
| 1988 | 1946 (S) | 75 | B−H−B stretching |
| 2566 | | 107 | |
| 2601 | 2550−2600 (S) | 280 | B−H stretching |
| 2615 | | 532 | |
| | | $B_{10}H_{14}@Li$ | |
| 155 | | 486 | Li stretching |
| 330 | | 1025 | B−B skeleton bending |
| 698 | | 225 | B−H bending ∥ $C_2$ axis |
| 815 | | 426 | B−H bending ⊥ $C_2$ axis |
| 1122 | | 4786 | B−H−B stretching |
| 1476 | | 1599 | B−H−B stretching |
| 1940 | | 1105 | B−H−B stretching |
| 2593 | | 584 | B−H stretching |

[a] Experimental Raman frequency values of strongly active (S) modes from ref 15d.

in the NBO charge of the Li atom, resulting in a nonsignificant interaction of Li with $B_5H_9$. Similar small changes also have been observed with other borane clusters where the number of boron and bridging hydrogen atoms might be considered important structural parameters to determine this Li and borane interaction as has been explained in section 4 of the Supporting Information.

**Raman Spectra.** To gain insights into the structure−property relationship, Raman spectra of $B_{10}H_{14}$ and $Li@B_{10}H_{14}$ have been calculated at MP2/6-31+G* and are presented in Table 2 and Figure 3a. In the Raman spectrum of $B_{10}H_{14}$, there are five distinctive vibrations with relatively higher activity that lie at 339, 696, 861, 1988, and 2566−2615 $cm^{-1}$. These frequencies correspond to the characteristic vibration modes of the $B_{10}H_{14}$ basket and are in excellent agreement with the experimental[15d] Raman frequency of $B_{10}H_{14}$ as shown in Table 2. It is important to mention that although a higher activity often relates to a higher intensity, here the experimental comparison is only made among the frequency values of Raman-active modes. The vibrations of $B_{10}H_{14}$ have low activities below 550 au with the highest at 532 au which are related to the B−H stretching mode of $B_{10}H_{14}$. The Raman spectrum of $Li@B_{10}H_{14}$ shows some new peaks along with characteristic peaks of $B_{10}H_{14}$. These peaks are much higher in activity than those of $B_{10}H_{14}$, having a highest activity peak of 4786 au. This increase in Raman activity of about 9-fold in $Li@B_{10}H_{14}$ is very close to that of Li@calyx[4]pyrrole.[5b] Different types of modes assigned to these vibrations are presented in Table 2.

A careful analysis of these modes shows that all three highest Raman active vibration modes are related to bridging hydrogen atoms of $Li@B_{10}H_{14}$, which are inward, upward, and toward the central Li atom, respectively, resulting in an effective interaction of these bridging hydrogens with the lithium atom. At 330 $cm^{-1}$ the B−B skeleton bending vibration with significant inward displacement of terminal $B_6$ and $B_9$ atoms also shows an increase in its Raman activity from 8 to 1025 au, which is in accordance with the shortening of the distance between the $B_6$ and $B_9$ atoms, as has been explained in the prior section. A noticeable vibration in the Raman spectrum of $Li@B_{10}H_{14}$ is the stretching of the Li atom in and out of the open face of the $B_{10}H_{14}$ basket at 155 $cm^{-1}$ with a relatively medium activity of 486 au. The inward synchronizing stretching vibration of the four bridging hydrogens with highest activity and one associated with the stretching of the Li atom are shown in Figure 3b.

**$^{11}$B NMR Spectra.** The calculated $^{11}$B NMR spectra and shielding tensors for $B_{10}H_{14}$ and $Li@B_{10}H_{14}$ are presented in Figure 4 and Table 3. The $^{11}$B NMR spectrum of $B_{10}H_{14}$ is composed of four singlets that are consistent with apparent $C_{2v}$ symmetry. The experimental spectrum[20a] of $B_{10}H_{14}$ (inset) has also been reproduced. The agreement between experimental and computational results has given us confidence that the calculated $^{11}$B NMR shifts for $B_{10}H_{14}$ and $Li@B_{10}H_{14}$ are consequential for this work. The chemical shifts of the nuclei, for the boron atom, result from both diamagnetic and paramagnetic terms. The diamagnetic shielding leads to an upfield shift and is derived from just the ground-state charge distribution. The paramagnetic term that leads to the downfield shift results from the coupling of occupied and virtual orbitals by the perturbation of the applied magnetic field.[20b,c] A careful analysis of these spectra shows that the B(1, 5, and 6) groups of atoms in $Li@B_{10}H_{14}$ have higher shielding values and are upfield compared those in $B_{10}H_{14}$ (see Figure 4). In the $Li@B_{10}H_{14}$ complex, when the metal transfers electron density to the cluster, it fills in some vacancies (regions of charge depletion) in the electron-deficient cluster. This causes the LUMO to perhaps shift toward the metal center. Therefore, there are two results: the charge transfer back to the metal during the transition (HOMO to LUMO transition) and the upfield shifts in the $^{11}$B NMR. If the LUMO shifts to the metal center, then in the presence of a magnetic field, the areas of charge concentration, $\langle 0|$, and charge depletion, $|n\rangle$, will not be as easily connected by the angular momentum operator, denoted $|l_z|$ in the following equation:[21]

$$\sigma_{zz}^{p} = -\frac{e^2 u_0}{4\pi {m_e}^2} \sum_n \frac{\langle 0|l_z|n\rangle}{E_0 - E_n} \langle n|\frac{l_z}{r^3}|0\rangle \qquad (6)$$

(18) Frisch et al. *Gaussian 03*, revision C.02; Gaussian, Inc.: Pittsburgh, PA, 2003.
(19) (a) Bondi, A. *J. Phys. Chem.* **1964**, *68*, 441–452. (b) Rowland, R. S; Taylor, R. *J. Phys. Chem.* **1996**, *100*, 7384–7391.
(20) (a) Li, Y.; Carroll, P. J.; Sneddon, L. G. *Inorg. Chem.* **2008**, *47*, 9193–9202. (b) Saika, A.; Slichter, C. P. *J. Chem. Phys.* **1954**, *22*, 26–28. (c) Wiberg, K. B.; Hammer, J. D.; Keith, T. A.; Zilm, K. *J. Phys. Chem. A* **1999**, *103*, 21–27.

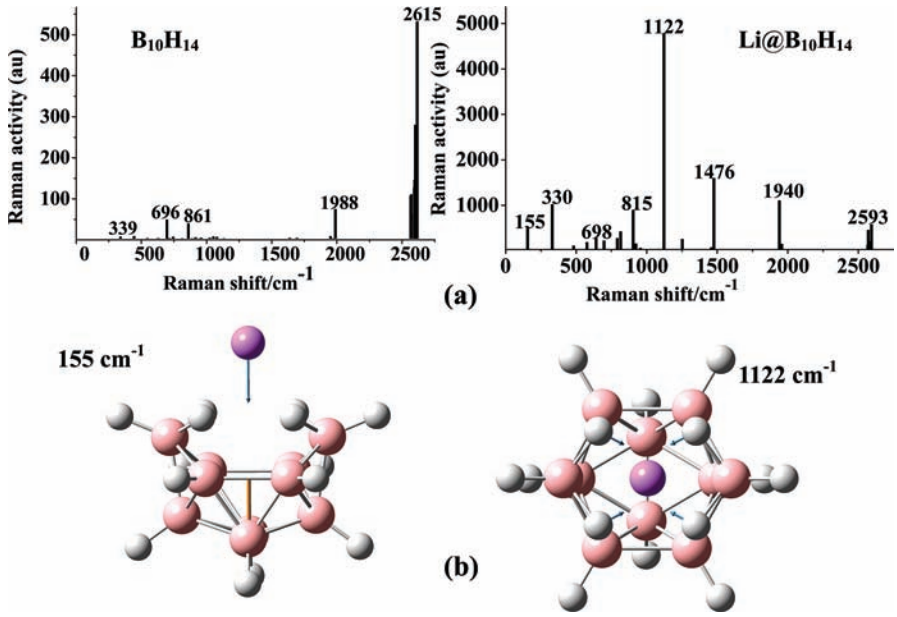


***Figure 3.*** (a) Raman spectra of $B_{10}H_{14}$ and Li@$B_{10}H_{14}$. (b) Raman high-activity vibration modes related to the Li atom and bridging H atoms.

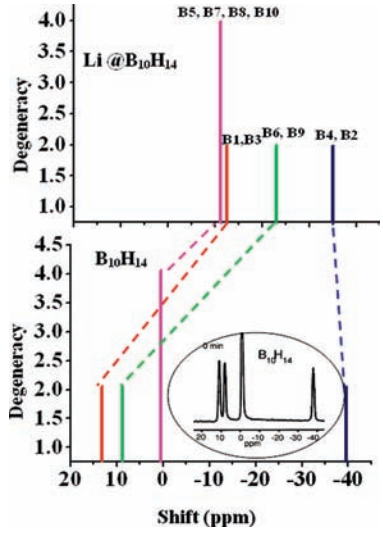


***Figure 4.*** $^{11}$B NMR spectra of $B_{10}H_{14}$ and Li@$B_{10}H_{14}$. The inset experimental spectrum of $B_{10}H_{14}$ is reprinted from ref 20a. Copyright 1999 American Chemical Society.

***Table 3.*** Diamagnetic ($\sigma^d$), Paramagnetic ($\sigma^p$), and Isotropic ($\sigma_{iso}$) Shielding Tensors (ppm) for $B_{10}H_{14}$ and Li@$B_{10}H_{14}$

| shielding tensor | B(5) group B5, B7, B8, B10 | B(1) group B1, B3 | B(6) group B6, B9 | B(2) group B2, B4 |
|---|---|---|---|---|
| | | $B_{10}H_{14}$ | | |
| diamagnetic | 207.58 | 207.70 | 210.73 | 210.12 |
| paramagnetic | −87.69 | −100.39 | −99.09 | −49.54 |
| isotropic | 119.88 | 107.30 | 111.64 | 160.17 |
| | | Li@$B_{10}H_{14}$ | | |
| diamagnetic | 204.10 | 206.02 | 212.53 | 200.55 |
| paramagnetic | −72.28 | −73.00 | −68.71 | −44.73 |
| isotropic | 131.82 | 133.00 | 143.81 | 155.81 |

Therefore, even though the HOMO−LUMO energy gap is lower ($E_0 - E_n$ term), they are now no longer in the correct orientation/proximity to provide a large overlap ($\langle nll_z/r^3|0\rangle$ term). Thus, we get less deshielding by the paramagnetic term (less negative number) and a subsequent upfield shift for the B(5, 1, and 6) groups of atoms in Li@$B_{10}H_{14}$.

***Table 4.*** Dipole Moments ($\mu$), Difference in the Dipole Moment ($\Delta\mu$) between the Ground State and Excited State, HOMO−LUMO Gap Energy, and Vertical Ionization Potential (VIP) Along with the Static Polarizability ($\alpha$), Hyperpolarizability ($\beta_0$), and Frequency-Dependent Hyperpolarizability ($\beta_\omega$) Values for Different Chemical Models at the MP2/6-31+G* Level of Theory

| property | $B_{10}H_{14}$ | Li@$B_{10}H_{14}$ | $Li^+$@$B_{10}H_{14}$ |
|---|---|---|---|
| $\mu$ (au) | 1.21 | 3.59 | 5.31 |
| $\alpha$ (au) | 120 | 186.00 | 124 |
| $\beta_x$ (au) | 0.13 | 90.00 | 0.60 |
| $\beta_y$ (au) | 0.51 | 900.00 | 9.60 |
| $\beta_z$ (au) | 67.80 | 23058.00 | 99.60 |
| $\beta_0$ (au) | 68.00 | 23075.00 | 100 |
| $\beta_\omega{}^c$ (au) | 180.53 | 26430.00 | |
| $\Delta\mu$ (au) | 0.224 | 1.297 | |
| ΔH−L (eV) | 11.05 | 5.21 | |
| VIP (eV) | 10.21 (10.10)[a] (10.50)[b] | 6.12 (6.64)[a] | |

[a] B3LYP/6-31+G*. [b] Experimental value from ref 15f. [c] $\beta(-2\omega;\omega,\omega)$ at $\omega = 0.0720$ au.

**Static First Hyperpolarizability ($\beta_0$).** The electric properties of $B_{10}H_{14}$ and Li@$B_{10}H_{14}$ calculated with the MP2 method are given in Table 4. It can be found that there are some great differences in the electric properties of both the systems. The dipole moment and polarizability of $B_{10}H_{14}$ are 1.21 and 120 au, while those of Li@$B_{10}H_{14}$ are 3.59 and 186 au, respectively. Furthermore, the most interesting change is in the first hyperpolarizability, which has become our focus of attention. The $\beta_0$ value of $B_{10}H_{14}$ is only 68 au. Due to the lithiation effect in $B_{10}H_{14}$, this $\beta_0$ value of 68 au dramatically mounts into a value of 23075 au for Li@$B_{10}H_{14}$ with a remarkable increase of 339-fold. Li@$B_{10}H_{14}$ with a cagelike inorganic complexant has registered a considerably large $\beta_0$ value of 23 075 au, which is 3 times and 2 times larger than those of Li@calyx [4]pyrrole[5b] and $Li^+$(calyx[4]pyrrole)$Li^-$,[5i] respectively. Besides this, the

(21) (a) Ramsey, N. F. *Phys. Rev.* **1950**, *78*, 699–703. (b) Wiberg, K. B.; Hammer, J. D.; Zilm, K. W.; Cheeseman, J. R.; Keith, T. A. *J. Phys. Chem. A* **1998**, *102*, 8766–8773. (c) Wiberg, K. B.; Hammer, J. D.; Keith, T. A.; Zilm, K. W. *J. Phys. Chem. A* **1999**, *103*, 21–27.

***Table 5.*** Transition Energies ($\Delta E$) and Oscillating Strengths ($f_0$) for $B_{10}H_{14}$ and $Li@B_{10}H_{14}$

| transition | $\Delta E$ (eV) | $f_0$ | major contribution | $C_i^b$ |
|---|---|---|---|---|
| | | $B_{10}H_{14}$ | | |
| $S_0 \rightarrow S_1$ | 5.741 (4.760)[a] | 0.100 | H → L | 0.64 |
| $S_0 \rightarrow S_2$ | 6.467 | 0.026 | H − 1 → L | 0.62 |
| $S_0 \rightarrow S_3$ | 6.837 | 0.004 | H − 2 → L | 0.63 |
| | | $Li@B_{10}H_{14}$ | | |
| $S_0 \rightarrow S_1$ | 1.549 | 0.111 | H → L | 0.93 |
| $S_0 \rightarrow S_2$ | 2.494 | 0.031 | H → L + 5 | 0.73 |
| $S_0 \rightarrow S_3$ | 3.208 | 0.072 | H → L + 6 | 0.77 |

[a] Experimental value from ref 15e. [b] Configuration interactions.

change in the $\beta_0$ value of about 339-fold due to the lithiation effect is also higher than those of several reported Li electride complexes.[5a,b,e−g,i,j]

Why is the $\beta$ value of $Li@B_{10}H_{14}$ much larger than that of $B_{10}H_{14}$? To gain an understanding of the origin of the $\beta_0$ values, we consider the widely used two-level model[22]

$$\beta_0 = {}^3/_2\Delta\mu f_0/\Delta E^3 \quad (7)$$

where$\Delta E$, $f_0$, and $\Delta\mu$ are the transition energy, oscillator strength, and difference in the dipole moments between the ground state and the crucial excited state. In the two-level expression, the third power of the transition energy is inversely proportional to the $\beta_0$ value. The transition energy is the decisive factor in the first hyperpolarizability. The transition energies of two species, $B_{10}H_{14}$ and $Li@B_{10}H_{14}$, are obtained by the CIS method. Table 5 shows the first three transitions along with their major contributing molecular orbitals. The transition energy of the crucial transition, i.e., the first transition with the lowest energy and highest oscillating strength, is 5.741 eV for $B_{10}H_{14}$ and 1.549 eV for $Li@B_{10}H_{14}$ which is close to those of 1.295−1.982 eV for the electride complexes, i.e., Li-doped fluorocarbon[5f] and crown ethers.[5b] This is the same as the case for the other two transitions that have lower energies and higher oscillating strengths for $Li@B_{10}H_{14}$. Because the transition energy of $Li@B_{10}H_{14}$ is much smaller than that of $B_{10}H_{14}$, according to the two-level model, it is reasonable that the $\beta_0$ value of 23 075 au in $Li@B_{10}H_{14}$ is much larger than that of 68 au in $B_{10}H_{14}$.

Besides this, we have roughly estimated the difference in the dipole moment between the ground state and first excited state through the CIS method, which is 0.224 au for $B_{10}H_{14}$ and 1.297 au for $Li@B_{10}H_{14}$. Thus, all three factors involved in the two-level model contribute to the large $\beta_0$ value of $Li@B_{10}H_{14}$. The Li atom is a highly polarizable system.[23] However, it is well-known that the $\beta_0$ value of the Li atom itself is close to naught. To show the sole contribution of the Li diffuse electron to the $\beta_0$ value of $Li@B_{10}H_{14}$, some electronic properties of $Li^+@B_{10}H_{14}$ also have been calculated and are given in Table 4. The $\beta_0$ value of $Li^+@B_{10}H_{14}$ at 100 au is close to the $\beta_0$ value of $B_{10}H_{14}$. This clearly indicates that the sole contribution to the larger $\beta_0$ value of $Li@B_{10}H_{14}$ is from the Li diffuse electron, in a manner somewhat similar to that in Li electride complexes with large NLO values.[5] Besides the static first hyperpolarizability, we have also estimated MP2 frequency-dependent $\beta(-2\omega;\omega,\omega)$ values at $\omega = 0.720$ au, which are 180.53 and 26430 au for $B_{10}H_{14}$ and $Li@B_{10}H_{14}$, respectively. The comparison with their $\beta_0$ values shows that the frequency-dependent effect is weak for $Li@B_{10}H_{14}$ but for $B_{10}H_{14}$ this effect is significant at $\omega = 0.720$ au. At lower frequency values both the systems, i.e., $B_{10}H_{14}$ and $Li@B_{10}H_{14}$, have shown a similar weak frequency-dependent effect as given in Table S4 of the Supporting Information. To compare the stability perspectives with those of previously reported works,[5] we have also calculated the vertical ionization potential (VIP) for $B_{10}H_{14}$ and $Li@B_{10}H_{14}$ (see Table 4) with the same reported methods. The VIP of 6.12 eV for $Li@B_{10}H_{14}$ is significantly larger than those of some previously reported Li organic electride complexes, such as Li@calyx[4]pyrrole (4.16 eV),[5b] $(Me)_3NH^+Na^-$ (3.904 eV),[5e] $Li^-$[15]aneN$_5$ (2.32 eV),[5c] ($Li^+@n^6$adz)$Li^-$ (2.88 eV),[5j] and coordinated inorganic $Li(NH_3)_4Na$ (3.27 eV).[5a] Only $Li\cdots(HCN)_3$ has a VIP (5.95 eV)[5g] comparable to that of $Li@B_{10}H_{14}$ with a similar configuration, i.e., a terminal H atom as a pulling group and the Li atom as an electron donor, which confirms our concept that the inward pull has provided more stability to the Li diffuse electron. From Table 4, $Li@B_{10}H_{14}$ shows a large HOMO−LUMO energy gap of 5.21 eV, which is significantly larger as compared with the HOMO−LUMO energy gaps of 2.16 eV in $Li^-$[15]aneN$_5$[5c] and about 1.85 eV in $AdzLi^+Na^-$.[5e] It also suggests that $Li@B_{10}H_{14}$ has reasonably good thermal stability. Definitely, this is due to the inward pull of the $B_{10}H_{14}$ basket, which has perhaps imparted greater stability to the Li diffuse valence electron[5g] and also has an additional advantage of its inorganic nature. Similarly, an inline trend in the analysis of potential energy profiles (PEPs) of different Li−borane complexes has been seen, in which an increase of the inward pull causes an increase of the thermal stabilities of the products (see section 5 of the Supporting Information for a detailed discussion about PEPs).

**Frontier Molecular Orbital Analysis.** In Scheme 1, we have presented the frontier molecular orbitals (FMOs) of $B_{10}H_{14}$ and $Li@B_{10}H_{14}$ involved in their first three lowest energy transitions. For $B_{10}H_{14}$, the LUMO is delocalized over all six atoms on the open face of the $B_{10}H_{14}$ basket with significant components at $B_6$ and $B_9$. This is consistent with the experiment in that $B_6$ and $B_9$ of $B_{10}H_{14}$ are susceptible to nucleophilic attack.[15c] Vividly, the HOMO density for $Li@B_{10}H_{14}$ has delocalization similar to that in the LUMO of $B_{10}H_{14}$, which has strengthened our assumption about the formation of a charge transfer complex between the Li atom and $B_{10}H_{14}$ basket.

As the lowest energy transition is from the HOMO to the LUMO for both $B_{10}H_{14}$ and $Li@B_{10}H_{14}$, we focus our attention especially on these orbitals. It has been examined that the principal coefficients for the HOMO of $B_{10}H_{14}$ have come from 2p orbitals of all boron atoms except for the B(1) group of atoms with small coefficients. The LUMO of $B_{10}H_{14}$ has significant mixing of 2p orbitals from the B(6) and B(2) groups of atoms and small coefficients from 2p orbitals on the B(5) group of atoms. The HOMO composition of $Li@B_{10}H_{14}$ consists of (about 60%) lithium diffuse s orbitals (3s and 4s) with relatively larger and smaller coefficients from the 2p orbitals of the B(6), B(5), and B(1) groups of atoms. The LUMO of $Li@B_{10}H_{14}$ has a composition fairly similar to that of the HOMO but is situated to the opposite side of the Li atom away from the $B_{10}H_{14}$ basket, resulting in long-rang charge transfer. In a nutshell, from the orbital analysis, we can draw the following points about the formation of the $Li@B_{10}H_{14}$ complex. The open end of the $B_{10}H_{14}$ basket is electron deficient, largely due to the vacant p orbitals of the B(6) group of atoms. The Li atom ionizes because

(22) (a) Oudar, J. L.; Chemla, D. S. *J. Chem. Phys.* **1977**, *66*, 2664–2668. (b) Oudar, J. L. *J. Chem. Phys.* **1977**, *67*, 446–457.
(23) Politzer, P.; Jin, P.; Murray, J. S. *J. Chem. Phys.* **2002**, *117*, 8197–8202.

***Scheme 1.*** Frontier Molecular Orbitals with Their Energies (eV) and Configuration Interactions ($C_i$) in Crucial Transitions for $B_{10}H_{14}$ and Li@$B_{10}H_{14}$

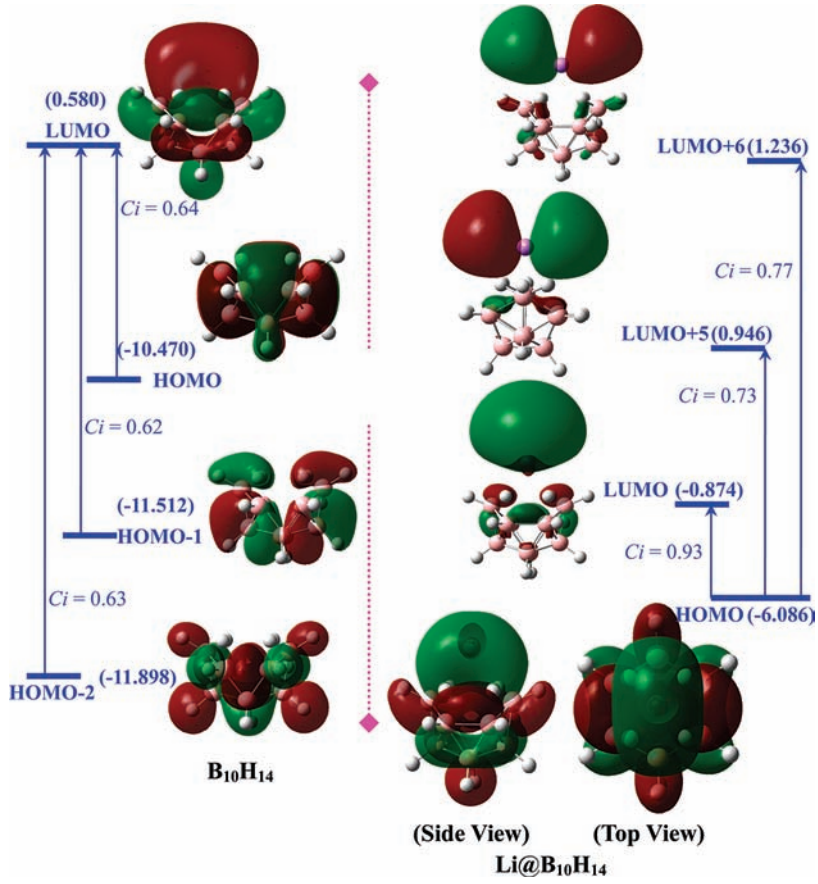


its loosely bound valence electron density is pulled into these empty orbitals or electron-deficient sites, which is further confirmed by the gain of −0.184e charge at this B(6) group of atoms during the formation of the Li@$B_{10}H_{14}$ complex. In Li@$B_{10}H_{14}$, the valence electron of the Li atom is diffused over the open end of the $B_{10}H_{14}$ basket (Scheme 1), which is easily excited to its Rydberg- and P-type LUMOs with lower transition energies and showed a remarkably large NLO response.

To gain a more comprehensive understanding and for the broad readership of our research work, we have probed the role of other metals doping with $B_{10}H_{14}$ and also other boranes and borane derivatives with a Li atom. We have doped $B_{10}H_{14}$ with different metals, i.e., Na, K, and Ca, and similarly a Li atom with different boranes and borane derivatives. These systems have been categorized in three sets as given in Table S5 of the Supporting Information. Among Na, K, and Ca, none of the metals could be effectively intercalated with the $B_{10}H_{14}$ basket to form a charge transfer complex with as remarkably large NLO properties as in the case of Li@$B_{10}H_{14}$. The preferable reactivity of Li toward the $B_{10}H_{14}$ basket might be due to its topological suitability at the open face of the $B_{10}H_{14}$ basket as has been explained in section 4 of the Supporting Information. The investigation with different boranes to intercalate with Li showed that higher numbers of boron and bridging atoms might be considered important parameters to bring higher charge transfer and stability in these Li−borane complexes. A more detailed discussion can be found about these systems in section 2 of the Supporting Information. Similarly, in set III of Table S5, some derivatives of decaborane have been reported which are based on previous experimental[15c] and theoretical[7b] work. Among these derivatives, the $\beta_0$ values of Li@2,4-$F_2B_{10}H_{12}$ and Li@2,4-$I_2B_{10}H_{12}$ are 14 331 and 16 623 au, respectively. Although these $\beta$ values are not remarkably large, these derivatives have higher dipole moments and VIPs, which might be attributed to the downward pull provided by the halo atoms from the 2 and 4 positions of the basket.

Finally, in wrapping up our above discussion, we have made some predictions that might be tested by experimentalists or theorists in the future.

(1) The lithiation of $B_{10}H_{14}$ may be obtained by the addition of lithium at the open end of the decaborane basket, and the product might be identified with higher Raman activity and/or at higher shielding values of $^{11}$B NMR especially for $B_6$ and $B_9$ atoms at the open end of Li@$B_{10}H_{14}$.

(2) The inorganic nature of Li@$B_{10}H_{14}$ might be helpful for experimentalists to handle it at room temperature and/or to use experimental conditions which are not possible with organic compounds.

(3) Li@$B_{10}H_{14}$ can be used as a functional material with a remarkably large electro-optical response.

(4) As the key to the formation of organic electrides is that alkali-metal atoms are captured and ionized by complexants to form cations and excess electrons,[5b] Li@$B_{10}H_{14}$ also might be checked as a new candidate having electride-like characteristics with considerable stability.

(5) The effective halo substitution at the 2- and 4-boron atoms can tune the stability and NLO character of the Li@$B_{10}H_{14}$ basket. Other combinations of halo substitutions besides at the 2 and 4 positions can also be checked to get a trade-off between

the remarkably large NLO property and higher stability of these fluoro derivatives.

Further study along this line is in progress in our laboratory to find the optimum substitution positions on this $Li@B_{10}H_{14}$ basket.

## Conclusions

We have studied the interaction of a Li atom with the $B_{10}H_{14}$ basket. The Li atom has shown an effective interaction among the other alkali metals and is bound in a handle fashion to the polar end of the $B_{10}H_{14}$ basket. In our results, the intercalation of the Li atom has produced a remarkable enhancement of the nonlinear optical response. Transition energies and FMO analysis have shown that the valence electron of the Li atom is diffused and easily excited. The transition energy of the crucial excited state for $Li@B_{10}H_{14}$ becomes quite small, resulting in a remarkably large $\beta_0$ value. The present Li complex has two advantages over the previously designed electride complexes: the use of an inorganic rigid complexant to impart greater thermal stability and the inward pull of the $B_{10}H_{14}$ basket, binding the diffuse electron more tightly without diminishing its large NLO values, which is an advantage for its experimental study. Furthermore, the 2,4-halo derivatives have further enhanced the stability of this $Li@B_{10}H_{14}$ with significantly large $\beta_0$ values. Besides this, the intercalation of lithium with decaborane has shown some fascinating effects on its Raman, $^{11}B$ NMR, and UV−vis spectra, which might be helpful for experimentalists to find this inorganic complex with large NLO properties.

**Acknowledgment.** We gratefully acknowledge financial support from the National Natural Science Foundation of China (Project No. 20703008), Chang Jiang Scholars Program (2006), Program for Changjiang Scholars and Innovative Research Team in University (Grant IRT0714), National Basic Research Program of China (973 Program-2009CB623605), Training Fund of NENU's Scientific Innovation Project (Grants NENU-STC07047, -STC08005, and -STC08012), and Science Foundation of Young Teachers of Northeast Normal University (Grant 20090402). S.M. also acknowledges the China Scholarship Council (CSC) and Ministry of Education, Government of Pakistan, for the award of a scholarship in the Ph.D. program. We are also thankful to Dr. L. E. Johnson at the University of Louisville for his useful discussion about $^{11}B$ NMR calculations.

**Supporting Information Available:** Complete ref 18, effect of the basis set on the first hyperpolarizability, TD-DFT calculations, different frequency-dependent first hyperpolarizabilities, $B_{10}H_{14}@Li$-based chemical models, potential energy profiles, and optimized Cartesian coordinates of $B_{10}H_{14}$ and $Li@B_{10}H_{14}$. This material is available free of charge via the Internet at http://pubs.acs.org.

JA9032023